

Received: 25 February 2018 / Accepted: 15 April 2018 / Published online: 25 June 2018

*heat transfer control, capillary-porous coatings,  
natural mineral media, heat-transfer crisis,  
capillary-porous system, thermal power plants*

Alexander A. GENBACH<sup>1</sup>  
David Yu. BONDARTSEV<sup>1</sup>  
Iliya K. ILIEV<sup>2\*</sup>

## **INVESTIGATION OF A HIGH-FORCED COOLING SYSTEM FOR THE ELEMENTS OF HEAT POWER INSTALLATIONS**

The studies of the ultimate thermal flows have been carried out in metallic and poorly heat-conducting porous structures, which operate when gravitational and capillary forces act jointly and cool various devices of thermal power plants in order to create a scientific methodology. The mechanism of destruction of metal vaporizing surfaces and poorly heat-conducting coatings of low porosity made of natural mineral media (granite) has been described on the basis of the problem of thermoelasticity and experimental data. Thermal flow dependences on time of their action and depth of penetration of temperature perturbations were identified based on analogy. Capillary-porous systems have high intensity, heat transport ability, reliability, compactness. The results of calculations and experiment showed that the maximum thickness of the particles that detach under the influence of compression forces for granite coatings is  $(0.25\div 0.3)\cdot 10^{-2}$  m. Sections of compression curves that determine the detachment of particles with dimensions of more than  $0.3\cdot 10^{-2}$  m for large thermal flows and short feed times, are screened by the melting curve, and in the case of small thermal flows and time intervals – the expansion curve.

### **1. INTRODUCTION**

Successful use of capillary-porous materials in engineering attracted many researchers and inventors to create different devices on their basis. The intensity of heat-eliminating systems and the forcing of processes taking place therein increased [1-2]. In addition to cooling systems, the use of porous materials allowed the creation of units which addressed the problems of explosion safety, labor protection and durability. This was facilitated by the ability to control evaporation processes due to excess fluid in pores and capillary structures, formed by the combined action of capillary and mass forces.

In thermal power plants (TPPs), capillary-porous materials are used to cool highly-forced detonation burner units, to create steam coolers in steam boilers, oil coolers that prevent oil from entering cooling water and water from entering the bearing system and

---

<sup>1</sup> Almaty University of Power Engineering and Telecommunications, Department of Heat Engineering Installations, Almaty, Kazakhstan

<sup>2</sup> University of Ruse, Department of Thermotechnics, Hydraulics and Ecology, Ruse, Bulgaria

\* E-mail: [iiliev@enconservices.com](mailto:iiliev@enconservices.com)

DOI: 10.5604/01.3001.0012.0937

labyrinth seals, and are used in other devices. The main areas of practical application of capillary-porous systems are presented in [3, 4].

The main advantages of capillary-porous systems include high intensity, high heat transport ability, reliability, compactness, simplicity in manufacture and operation. These systems improve operational and technological performance and have low capital and operating costs. Based on the study of capillary-porous systems, new technical solutions have been developed to improve the performance characteristics of the thermal power plant in relation to the powerful power units of combined heat and power plants.

The authors of [5] carry out a comparative analysis of methods for calculating the heat transfer, based on the water boiling with underheating in vertical channels, and they consider that the hot spot corrosion of fuel element claddings of nuclear reactor fuel elements is similar to the capillary-porous structure [6, 7]. It is interesting to make an analogy using the turbulence model. However, no studies of heat transfer through a regular structured surface have been carried out.

According to the authors' opinion [8, 9], surface boiling on porous surfaces can influence the development of corrosion due to the erosive action on the heat exchange surface, when the bubbles of steam fall in an underheated liquid. Therefore, it is required to investigate the evaporation of liquid in capillary-porous structures in the field of capillary and mass forces, taking into account the velocity and underheating, which are formed by excess fluid.

Of particular interest is the comparison between the intensity of the heat transfer and the critical condition of the surface (boiling crisis) of the heat pipes [10, 11]. An assessment of the capabilities of the mechanics for the destruction of the heating surfaces (cooling) covered in capillary-porous bodies has been carried out. All this can be used in the assessment of the strength and the resource potential of thermal-mechanical equipment of power stations, as well as for justification of their safety when used [12, 13]

An estimated intensity of heat transfer for liquid boiling in a large volume and thin films on a smooth surface showed equal possibilities [5-7] at high thermal flow and higher heat transfer parameters than that in systems with a capillary-porous coating [14, 15]. It is required to carry out investigations of the heat transfer capabilities of capillary-porous coatings operating in the field of capillary and mass forces, and to establish ultimate (critical) load values leading to the destruction of the heating surfaces. Figure 1 presents a method for studying capillary-porous systems for various elements of power plants. The systems differ in the fact that they have predominantly a gravitational fluid supply and occupy an intermediate position between thin-film evaporators and porous evaporators with a predominantly capillary fluid supply (heat pipes) in terms of the intensity of heat transfer. Therefore, such systems should be identified in a separate class of heat-eliminating systems. The performed research makes it possible to give recommendations on the selection of the heating-and-cooling medium, taking into account the type of its circulation, determining the geometry and material of apparatuses and heat exchange intensifiers, considering the conditions and orientations of the system operation under pressure or underpressure, the energy supply and type and the system orientation. Generalization of the experimental results and calculation procedure for heat and mass transfer in capillary-porous systems in accordance with Figure 1, are presented in [3, 4].

The investigation of various factors affecting the heat transfer in the structures show that the critical states of the heating surface are of particular interest, when the system is capable of carrying the maximum flows of energy and substance. In this case, however, the values of thermal flows and thermal stresses are required to be known in order to ensure a reliable long-term operation of the unit. Consequently, the maximum energy and substance transfer can be obtained for the following conditions: a pure liquid circulating in a forced scheme in closed elliptical heat exchangers under pressure in perforated and profiled heating surfaces made of stainless steel is used. The system operates with an excessed fluid, and the presence of mass forces ensures the forced flow of the heating-and-cooling medium with underheating. Energy is supplied to the vertical surface along the perimeter, with a supersonic high-temperature pulsating rotating torch [1, 2]. Mathematical models of turbines are useful when the impact of their installation on a foundation, especially in seismic zones, for example in the vicinity of Almaa [16] is considered. An article [17] presents a phase transition model created with software programs for accurately prediction the changes occurring during cooling, especially in the non-uniform temperature field, which affect the phase transformations and ultimately the residual stresses.

## 2. AN EXPERIMENTAL METHOD FOR STUDYING THE HEAT TRANSFER CRISIS AND THE CRITICAL STATE OF A HEAT EXCHANGE SURFACE COATED WITH A CAPILLARY-POROUS MEDIUM

Experimental units allowing to investigate the following integral characteristics of heat transfer have been developed: ultimate thermal flows ( $q$ ), up to critical ones; liquid ( $m_l$ ) and vapor ( $m_v$ ) flow rates; distribution of the temperature field along the height and the length of the heat exchange surface. Studies are carried out in a capillary-porous cooling system which can operate on the principle of a closed evaporative-condensation design, or to be open. Various heat exchange conditions are studied, including: method of the coolant supply; the extent of tightness of the capillary-porous structure; ability to feed up the micro-arterial structure along the height of the heat exchange surface; orientation of the surface relative to gravitational forces; geometry: flat, tubular and curved cooling surfaces; influence of pressure up to manifestations of crisis with wall burning (see Fig. 1). To study the mechanism of heat transfer, holography methods and the generalization of similar and analogous phenomena are used [1-4]. The heat exchange is controlled using the elliptical systems, by the combined action of capillary and mass forces [1, 2]. The study of heat transfer is of a practical nature. It is intended for the creation of various thermal power plants: steam attemperators of steam boilers, porous coatings of poorly heat-conducting material, seals in steam turbines and a number of other power plants [1, 2].

Figure 2 shows a cross section of a flat experimental unit with a perforated pressure plate 3 (Fig. 3), tubular arteries 4 and a capillary-porous structure 2. The heat source in the experiment was electrical energy supplied through a low-voltage transformer. The specific heat flows varied within the range of  $10^4 - 2 \cdot 10^6$  W/m<sup>2</sup>. The adjustment of the heat flow was controlled by changing the voltage current.

The maximum possible error:

- A)  $\pm 0,6\%$ , when measuring current;  $\pm 1\%$ , when voltage is dropped; power is  $\pm 1,6\%$ ,  
 B)  $\pm 3\%$ , when determining the liquid flow rate, using a rate-of-flow meter.

The imbalance of the current-supplied heat and the heat led to circulation and excess water, taking into account heat losses through the insulation, did not exceed  $\pm 12\%$ , and  $\pm 11\%$  through circulating water. The discrepancy between the material balance between the flow rate of the cooling liquid and drainage and condensate flow is no more than  $\pm 10\%$ . The measurement procedure and the processing of experimental data were published in [4].

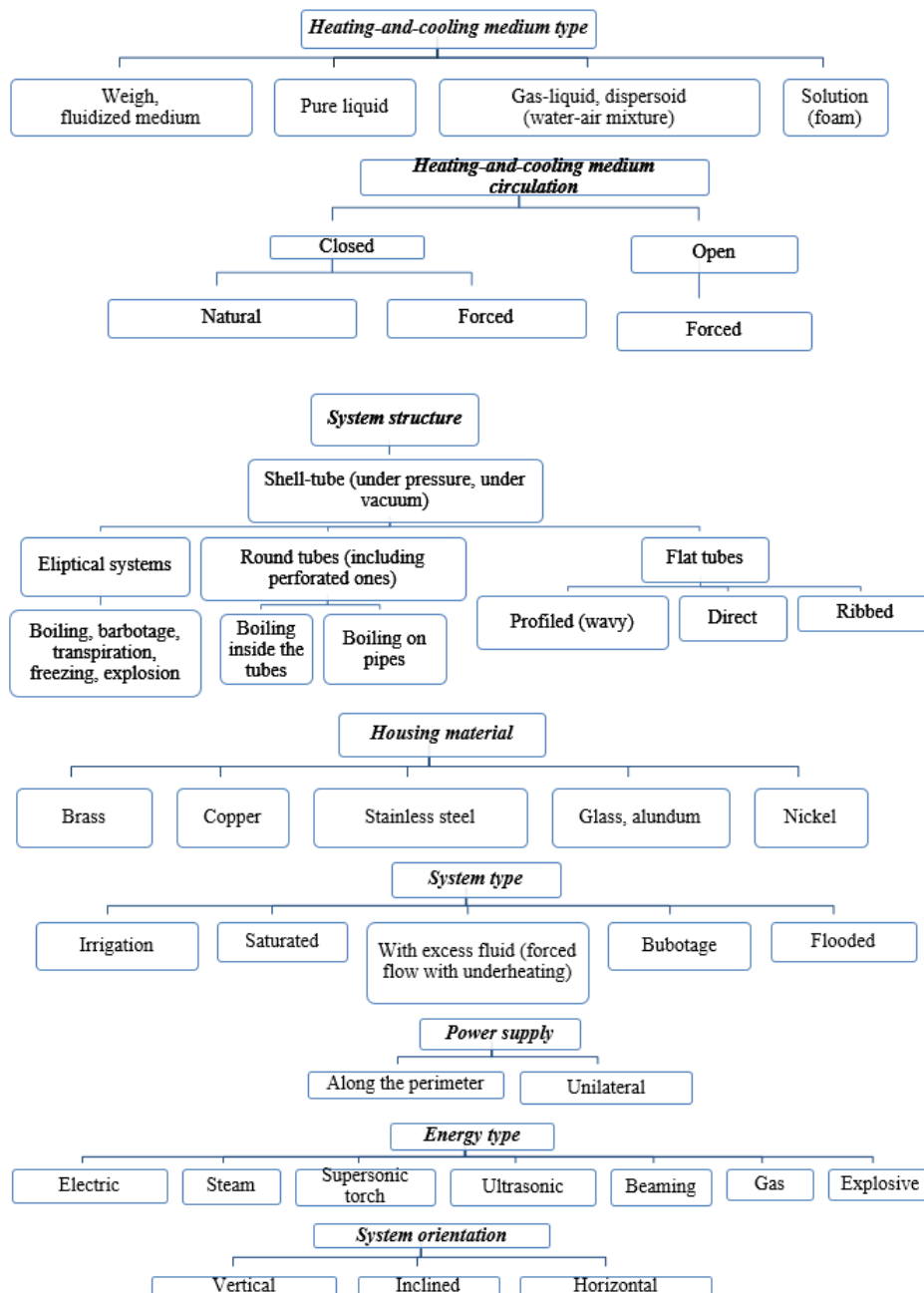


Fig. 1. A method for investigating various factors affecting the heat and mass transfer in capillary-porous systems of heat power installations

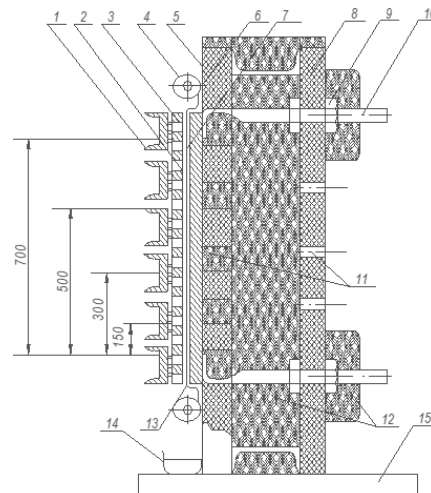


Fig. 2. Cross section of a flat experimental unit: 1–pressing bar, 2–capillary-porous structure, 3–perforated pressure plate, 4–tubular artery, 5–asbestos cement plate, 6–heater, 7–insulation, 8–plate, 9–clamping nut, 10– electrode, 11–windows, 12–heat insulation, 13–coolable wall, 14–collector, 15–stand

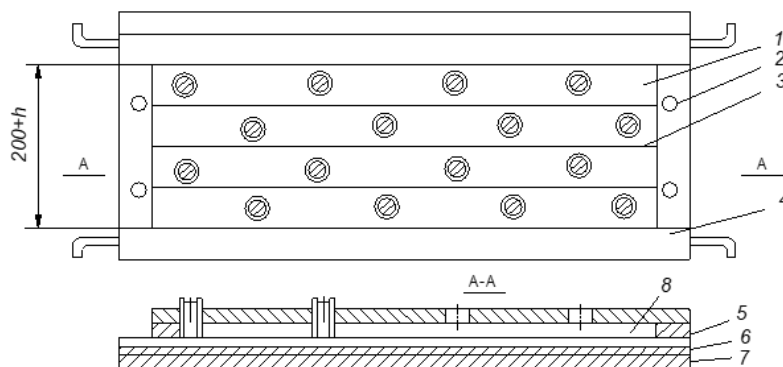


Fig. 3. Pressure scheme for the capillary-porous structure: 1 – plates, 2 – pressure screws, 3 – steam slots, 4–fluid supply, 5–pressure perforated plate, 6–capillary-porous structure, 7–heated wall, 8–microartery

To study the boiling crisis, we also assembled the units made in the form of a rocket-type flame-jet burner. The scheme of the experimental unit and the experimental conditions are presented in [2]. Ignition chambers and supersonic nozzles were cooled using a capillary-porous and water system (Fig. 4). The thermoreactive burner was also used to study the critical state of capillary-porous coatings made of natural mineral media (granite, quartz and teschenite coatings). The thermal effect was realized by a supersonic (up to 2000 m/s) high-temperature (up to 2500°C) pulsating torch (see Fig. 1, form of energy). Fig. 4 shows the results of the destroyed ignition chambers.

#### 2.1. RESULTS OF THE HEAT TRANSFER CRISIS IN THE CAPILLARY-POROUS COOLING SYSTEM AND THE DISCUSSION THEREOF

The results from the destruction of the combustion chambers and supersonic nozzles are shown in Fig. 4 with the following labels. a) nozzles are made without a wall thickening:

1, 2, 3, 4 – before operation; 5, 6 – after 40 hours of operation (the deflector rings are destroyed and nozzle cross-sections are enlarged); 1, 2, 5, 6 –  $\alpha=0.8$ ; 3, 4 –  $\alpha=0.6$ ; 4–ignition chambers with a shortened nozzle (this ensured the detonation combustion condition). Cooling system is water-operated ( $q_{ccs} = 1 \cdot 10^6 \text{ W/m}^2$ ;  $\bar{W} = 10 \text{ m/s}$ ); b) nozzles are made with a wall thickening: 1-8 –  $\alpha = 0.6 \dots 0.65$ , the destruction occurred as a result of the breakdown of gases into the water cooling system when the seals became depressurized; 5–ignition chamber with a fused swirled. Cooling system is capillary - porous ( $q_{ccs} = 1 \cdot 10^6 \text{ W/m}^2$ ).

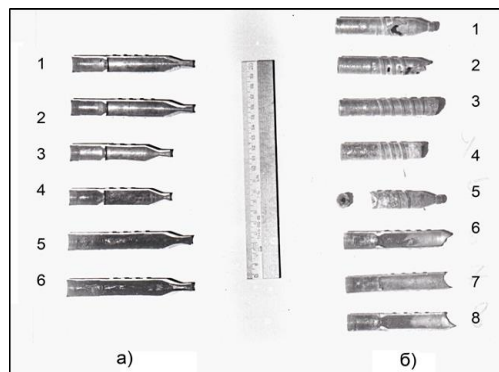


Fig. 4. Destroyed ignition chambers and supersonic burner nozzles

## 2.2. MODEL OF THE CAPILLARY-POROUS STRUCTURE OF THE COOLING SYSTEM

Figure 5 shows the model of a capillary-porous coating applied to the coolable surface of a heat-loaded element of power plants. At the onset of the boiling crisis, the critical state of the heating surface arises, and the latter is destroyed along with the coatings. Such a scheme allows to make a model of fissures of brittle coatings and plastic porous structures. The following labels are shown in Fig. 5. Straight lines – fluid movement; wavy lines – steam movement:  $q$  – thermal flow,  $T_g, T_w, T_s$  – temperatures of gases, walls and saturation;  $G_l(y), G_s$  – liquid and steam flow rates;  $\delta_w, \delta_{p.c.}, \delta_l, \delta_s$  – steam-generating surface, porous coating, liquid and vapor thicknesses  $b_z, d$  – width of porous coating cells and grain diameter.

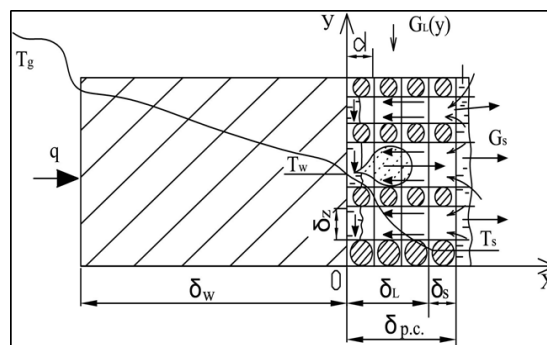


Fig. 5. Physical model of heat and mass transfer in a porous structure covering the coolable surface

### 2.3. MODEL OF A CAPILLARY-POROUS COATING FOR THE CRITICAL STATE OF THE HEATING SURFACE

To determine the critical thermal flows and stresses, the thermoelasticity problem [2] is solved under the secondary limiting conditions for the one-dimensional equation of nonstationary heat conductivity.

Let's consider a plate with the thickness of  $2h$ . The constant ultimate thermal flow  $q$  is supplied to the surface  $z = +h$ , starting from the timepoint  $t = 0$ . The bottom surface  $z = -h$  and the plate side edges are thermally insulated.

Thermal conductivity equation with limiting and initial conditions can be written in the form:

$$\begin{aligned} \alpha_w \frac{\partial^2 T}{\partial z^2} &= \frac{\partial T}{\partial \tau}, \quad T = 0, \quad \tau < 0; \\ \lambda_w \frac{\partial T}{\partial z} &= q, \quad z = +h; \\ \lambda_w \frac{\partial T}{\partial z} &= 0, \quad z = -h; \end{aligned} \quad (1)$$

The temperature distribution along the thickness depends on the thermophysical properties of the material, the thermal flow value and the feeding time:

$$T\left(\frac{z}{h}; \tau\right) = q \left\{ \frac{M}{2(c\lambda\rho)_w} \tau + \frac{3z^2 + \frac{6z}{h} - 1}{12M} - \frac{4}{\pi^2 M} \sum_{n=1}^{\infty} \frac{(-1)^n}{n^2} \exp\left[-n^2 \frac{\pi^2 M^2}{4(c\lambda\rho)_w} \tau\right] \cos\left[\frac{n\pi}{2} \left(\frac{z}{h} + 1\right)\right] \right\} \quad (2)$$

where  $M = \frac{\lambda_w}{h}$ ;  $n$  – positive numbers.

Using the known temperature distribution in the plate, we can find the thermal tension and compression stresses arising at a certain time  $t$  at various depths from the surface  $\delta_i = (h = z_i)$  for a given value of the thermal flow  $q$ , since the plate with a variable temperature is in the plain stress condition.

$$\sigma_{xx} = \sigma_{yy} = -\frac{\alpha E}{(1-\nu)} T\left(\frac{z}{h}; \tau\right) + \frac{1}{(1-\nu)2h} \int_{-h}^{+h} \alpha 2' ET\left(\frac{z}{h}; \tau\right) dz \quad (3)$$

where the first term is the component of the compression stress, and the second term is the tension stress.

*Solution to the equation (1)*

If we are given the limiting values of tension and compression stresses for the rock (porous coatings from the natural mineral medium) and the metal, we obtain the dependence of the thermal flow required for destruction on the time of delivery and the depth of penetration. In addition, equating the temperatures on the plate surface to the rock and metal melting temperature, we find the values of the ultimate thermal flows necessary for melting the surface layer for a different period of their action:

surface melting:

$$q_1 = \frac{T_f}{\left\{ \frac{M}{2(c\rho\lambda)_w} \tau + \frac{2}{3M} - \frac{4}{\pi^2 M} \sum_{n=1}^{\infty} \frac{(-1)^n}{n^2} \exp \left[ -n^2 \frac{\pi^2 M^2}{4(c\lambda\rho)_w} \tau \right] \cos n\pi \right\}} \quad (4)$$

$$q_2 = \frac{\frac{(1-\nu)\sigma_{ut}}{\alpha E}}{\frac{M}{2(c\rho\lambda)_w} \tau + \frac{3z^2}{h^2} + \frac{6z}{h} - 1 - \frac{4}{\pi^2 M} \sum_{n=1}^{\infty} \frac{(-1)^n}{n^2} \exp \left[ -n^2 \frac{\pi^2 M^2}{4(c\lambda\rho)_w} \tau \right] \left[ \cos \frac{n\pi}{2} \left( \frac{z}{h} + 1 \right) \right]} \quad (5)$$

creating ultimate tension stresses:

$$q_3 = \frac{\frac{(1-\nu)\sigma_{ut}}{\alpha E}}{\frac{M}{2(c\rho\lambda)_w} \tau} \quad (6)$$

The dependences of  $q_1$ ,  $q_2$ ,  $q_3$  on time  $\tau$  for fixed particle size  $\delta$  values for the coating, or the penetration depth of temperature perturbations for the metal, were calculated on a PC with respect to a plate made of quartz, granite and metal (copper and stainless steel).

### 3. MECHANISM AND CALCULATION OF THE CRITICAL STATE OF THE HEAT TRANSFER SURFACE. EXPERIMENTAL DATA ANALYSIS

The results of the calculations are shown in Figure 6-9. The maximum thickness of the particles that break off under the compression forces for granite coatings is  $(0.25-0.3) \cdot 10^{-2}$  m, which is in agreement with the results obtained by high-speed filming (Fig. 10).

Sections of the compression curves, which determine the breaking-off of particles with a size  $\delta > 0.3 \cdot 10^{-2}$  m for large thermal flows and small ones  $\tau$ , are screened with the melting curve, and in the case of small thermal flows and significant time intervals, they are screened with the expansion curve.

If vacancy cavities can be transformed into dislocations, the investigated coating obtain plastic properties and is not destroyed by the action of the torch. All metals are the same. Some rocks also have such property. The relationship between tension and compression stresses is stress diagrams within the plate for various time intervals from the beginning of the process under consideration. At small  $\tau$ , in the region of  $10^{-1}$  s, only compressive stresses arise. Starting from  $\tau \approx 1$  s, in some region  $\Delta(h-z_i)$  up to  $0.3 \cdot 10^{-2}$  m, the compression stresses turn into tension stresses in a very short period of time, and for different time intervals they are at different depth from the plate surface.

The upper limit of the stable destruction of the quartz coating is  $10^7$  W/m<sup>2</sup>, and that from granite is up to  $0.5 \cdot 10^7$  W/m<sup>2</sup>, and the lower limits, when there is still a detachment



of particles under the influence of thermal stresses of compression are  $0.25 \cdot 10^7 \text{ W/m}^2$  and  $0.05 \cdot 10^7 \text{ W/m}^2$ , respectively.

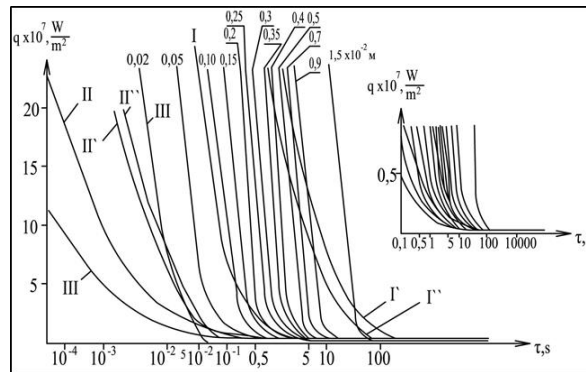


Fig. 6. Dependence of thermal flows causing compression stresses III of a granite coating according to the time of action  $\tau$  for different thickness  $\delta$  of the breaking-off particles: I – tension stresses sufficient for destruction ( $I', I''$  – copper and stainless steel,  $h = 0.1 \cdot 10^{-3} \text{ m}$ ); II – surface fusion ( $II', II''$  – copper and stainless steel,  $h = 0.1 \cdot 10^{-3} \text{ m}$ )

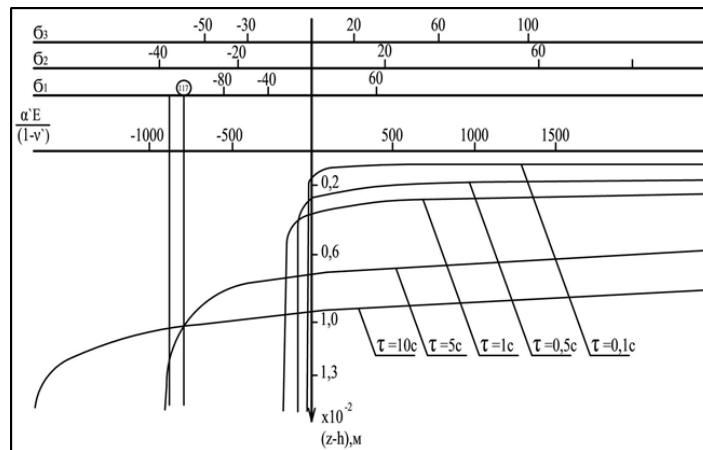


Fig. 7. Stress diagrams for the thickness of the limiting plate for different thermal flows and time of their action:  $q_1 = 0.142 \cdot 10^7 \text{ W/m}^2$ ;  $q_2 = 0.042 \cdot 10^7 \text{ W/m}^2$ ;  $q_3 = 0.075 \cdot 10^7 \text{ W/m}^2$ ; 117 – ultimate tension strength:  $\sigma, \cdot 10^5 \text{ H/m}^2$ ,  $E, \cdot 10^5 \text{ H/m}^2$

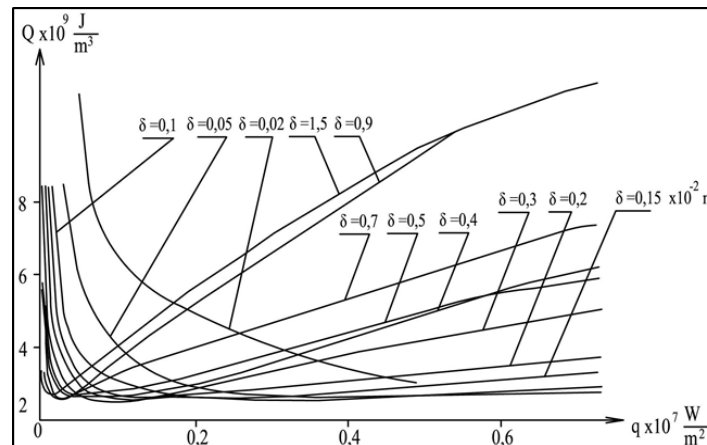


Fig. 8. Change in the ultimate destruction energy  $Q$  of the granite coating depending of  $q$  for various  $\delta$ ,  $Q = q \cdot \tau / \delta$

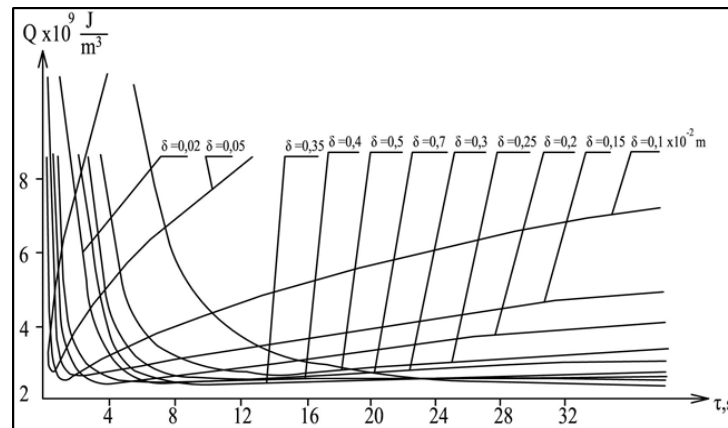


Fig. 9. Change in the ultimate destruction energy  $Q$  of the granite coating depending of  $\tau$  for various  $\delta$

The destruction of an anisotropic medium under the action of directional heating is based on the uneven expansion of its components (crystals). When increasing in volume, the heated layer of the coating rock starts to press adjacent less heated layers. Since the expansion in all other directions is hampered by the reaction of the unheated layers, the rock starts to expand freely from the open side and, due to its overextension, it separates and splits off.

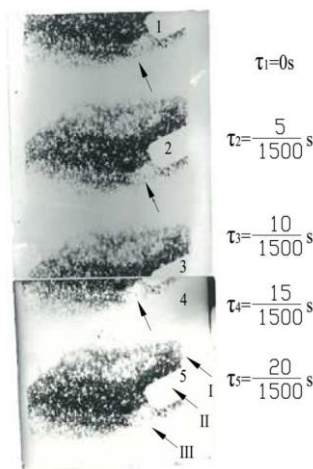


Fig. 10. A record of flight of husks with the size  $\delta = 2.5 \cdot 10^{-3}$  m when a granite coating particle is destroyed by a rocket-type burner ( $q = 1.2 \cdot 10^6$  W/m<sup>2</sup>): I – capillary-porous coating; II – burner axe, from which supersonic high-temperature, pulsating detonation gas flow flows out; III – a particle broken off from the coating

The testing was conducted with steam generating metal heating surfaces at the time of the boiling crisis. For metals, crystals are destroyed in directions up to  $10^{-5}$  V. The process of destruction consists of steps of initiation of fissures and their development. As a result of the thermal action microcracks are initiated in the region of stress concentrators (inclusions, inhomogeneities, fissures). High internal stresses can also arise due to inhomogeneous flow of plastic deformation, after which brittle failure occurs. In this regard, plastic deformation is considered as the primary cause of destruction, although it can

delay the growth of fissures. On the one hand, bond discontinuities due to thermal fluctuations are at the heart of the destruction, and on the other hand, destruction is a kinetic thermoactivation process, which is based on the displacement of vacancies to fissures, the growth of which determines the kinetics of destruction.

#### 4. CONCLUSION

Based on the conducted studies in case of exposure with a torch of a kerosene-oxygen burner of porous coating within working area, we have up to  $4 \cdot 10^7$  W/m<sup>2</sup> corresponded to  $q$  of coatings  $\approx 0.4 \cdot 10^7$  W/m<sup>2</sup>. The destruction mechanism of metals is fundamentally different from the rocks coatings' destruction mechanism. Despite this, thermal flow dependences on time of their action and depth of penetration of temperature perturbations were identified on the basis of analogy, which help to avoid the boiling crisis in the cooling system and ensure an optimal selection of porous coatings of low porosity and thermal conductivity. In the future, the studies of other porous natural materials are required.

A scientific method for studying and creating of capillary-porous cooling systems and coatings for various heat and mass transfer conditions in power equipment elements has been developed.

#### NOMENCLATURE

- $a$  – thermal conductivity factor, m<sup>2</sup>/s;
- $C$  – thermal capacity, J/kgK;
- $d$  – grain size (diameter) of the structure, m;
- $E$  – Young's modulus (elasticity modulus), Pa;
- $G$  – specific flow rate, kg/m<sup>2</sup>s;
- $h$  – film height, thickness, m;
- $m$  – flow rate, kg/s;
- $q$  – thermal load, W/m<sup>2</sup>;
- $Q$  – specific crushing energy, J/m<sup>3</sup>
- $T$  – temperature, K;
- $\bar{W}$  – average velocity, m/s;
- $w$  – grid cell width, inside-light inspection (hydraulic pore size), m;
- $x$  – coordinate (direction of fluid motion), m;
- $y$  – coordinate (direction of fluid motion), m;
- $z$  – coordinate, m;
- $\alpha$  – linear expansion factor, K<sup>-1</sup>;
- $\alpha$  – excess air factor;
- $\delta$  – thickness of the structure (depth of wave propagation, particles size), m;
- $\lambda$  – thermal conductivity factors, W/mK;
- $\nu$  – Poisson ratio (lateral contraction);
- $\tau$  – time, s;
- $\rho$  – density, kg/m<sup>3</sup>;
- $\sigma$  – stress.

#### Subscripts

f, v – fluid, vapor; ccs – critical cross-section; h – hot; w – wall; h – hydraulic; s – saturation; f – fusion (film); us – ultimate shortening; ut – ultimate tension.

## REFERENCES

- [1] POLYAEV V.M., GENBACH A.A., 1995, *Methods of monitoring energy processes, experimental thermal and fluid science*, International of Thermodynamics, Experimental Heat Transfer and Fluid Mechanics, Avenue of the Americas, New York, USA, 10, 273-286.
- [2] POLYAEV V.M. GENBACH A.A., 1991, *A limit condition of a surface at thermal influence*, Teplofizika Vysokikh Temperatur, 29, 923-934, (in Russian).
- [3] GENBACH A.A., JAMANKYLOVA N.O., BAKIC VUKMAN V., 2017, *The processes of Vaporization in the Porous Structures Working with the Excess of Liquid*, Thermal Science, 1, 21, 363-373.
- [4] GENBACH A.A., OLZHABAYEVA K.S., ILIEV I.K., 2016, *Boiling process in oil coolers on porous elements*, Thermal Science 5, 20, 1777-1789.
- [5] JAMIALAHMADI M., et al., 2008, *Experimental and theoretical studies on subcooled flow boiling of pure liquids and multicomponent mixtures*, Intern. J. Heat Mass Transfer, 51, 2482-2493.
- [6] OSE Y., KUNUGI T., 2011, *Numerical Study on Subcooled Pool Boiling*, Programme in Nuclear Science and Technology, 2, 125-129.
- [7] KREPPER E., et al., 2007, *CFD Modeling subcooled boiling-concept, Validation and Application to Fuel Assembly Design*, Nuclear Engineering and Design, 7, 716-731.
- [8] OVSYANIK A.V., 2012, *Modeling of processes of heat exchange at boiling liquids* (in Russian), Gomel State Technical University named after P.O., Sukhoy, Gomel, Belarus.
- [9] ALEKSEIK, O.S., KRAVETS V.Yu., 2013, *Physical model of boiling on porous structure in the limited space*, Eastern-European Journal of Enterprise Technologies, 64, 4/8, 26-31.
- [10] POLYAEV V.M., MAYOROV V.A., VASILEV L.L., 1998, *Hydrodynamics and heat exchange in porous structural elements of aircrafts*, Mechanical Engineering, 168, (in Russian).
- [11] KOVALEV S.A., SOLOVEV S.L., 1989, *Evaporation and condensation in heat pipes*, Science, 112, (in Russian).
- [12] KUPETZ M., JENI HEIEW E., HISS F., 2014, *Modernization and extension of the life of steam turbine power plants in Eastern Europe and Russia*, Heat power engineering, 6, 35-43, (in Russian).
- [13] GRIN E.A., 2013, *The possibilities of fracture mechanics in relation to the problems of strength, resource and justification for the safe operation of thermal mechanical equipment*, Heat Power Engineering, 1, 25-32. (in Russian).
- [14] SHKLOVER E.G., 1991, *Experimental study of heat transfer from porous surface in pool and forced – convection boiling at low pressures*, Phase Change Heat Transfer ASME, 159, 75-80.
- [15] BARTHAU G., 1992, *Active nucleation site density and pool boiling heat transfer*, Int. J. Heat Mass Transfer, 35, 271-278.
- [16] NOVOTNY L., SINDLER J., FIALA S., SVEDA J., 2016, *Modelling and Optimization of Machine Tools on Foundations*, Journal of Machine Engineering, 16/1, 43-56.
- [17] PERZYNSKI K., et al., 2016, *Numerical Evaluation of Gear Ring Behaviour During Various Cooling Conditions*, Journal of Machine Engineering, 16/2, 18-26.